

## Different evolution of the intrinsic gap in strongly correlated $\text{SmB}_6$ in contrast to $\text{YbB}_{12}$

This content has been downloaded from IOPscience. Please scroll down to see the full text.

2013 New J. Phys. 15 043042

(<http://iopscience.iop.org/1367-2630/15/4/043042>)

View [the table of contents for this issue](#), or go to the [journal homepage](#) for more

Download details:

IP Address: 192.108.69.177

This content was downloaded on 24/10/2013 at 11:33

Please note that [terms and conditions apply](#).

## Different evolution of the intrinsic gap in strongly correlated $\text{SmB}_6$ in contrast to $\text{YbB}_{12}$

J Yamaguchi<sup>1</sup>, A Sekiyama<sup>1,2</sup>, M Y Kimura<sup>1</sup>, H Sugiyama<sup>1</sup>,  
Y Tomida<sup>1</sup>, G Funabashi<sup>1</sup>, S Komori<sup>1</sup>, T Balashov<sup>3</sup>,  
W Wulfhekel<sup>3</sup>, T Ito<sup>4,5</sup>, S Kimura<sup>4</sup>, A Higashiya<sup>2,6</sup>, K Tamasaku<sup>2</sup>,  
M Yabashi<sup>2</sup>, T Ishikawa<sup>2</sup>, S Yeo<sup>7</sup>, S-I Lee<sup>8</sup>, F Iga<sup>9,10</sup>,  
T Takabatake<sup>9</sup> and S Suga<sup>1,2,11,12</sup>

<sup>1</sup> Graduate School of Engineering Science, Osaka University,  
Osaka 560-8531, Japan

<sup>2</sup> RIKEN SPring-8 Center, Kouto 1-1-1, Sayo, Hyogo 679-5148, Japan

<sup>3</sup> Physikalisches Institut, Karlsruhe Institute of Technology, D-76131 Karlsruhe,  
Germany

<sup>4</sup> UVSOR Facility, Institute for Molecular Science, Okazaki 444-8585, Japan

<sup>5</sup> Graduate School of Engineering, Nagoya University, Nagoya 464-8603, Japan

<sup>6</sup> Faculty of Science & Engineering, Setsunan University,  
Osaka 572-8508, Japan

<sup>7</sup> Korea Atomic Energy Research Institute, Daejeon 305-600, Republic of Korea

<sup>8</sup> Department of Physics, Sogang University, Seoul 121-742, Republic of Korea

<sup>9</sup> Graduate School of Advanced Sciences of Matter, Hiroshima University,  
Higashi-Hiroshima 739-8526, Japan

<sup>10</sup> Faculty of Science, Ibaraki University, Mito 310-0056, Ibaraki, Japan

<sup>11</sup> Max-Planck-Institute for Microstructure Physics, Weinberg 2,  
Halle D-06120, Germany

E-mail: [ssmsuga@gmail.com](mailto:ssmsuga@gmail.com)

*New Journal of Physics* **15** (2013) 043042 (12pp)

Received 18 November 2012

Published 23 April 2013

Online at <http://www.njp.org/>

doi:10.1088/1367-2630/15/4/043042

**Abstract.** Dependence of the spectral functions near the Fermi level on temperature and rare-earth atom doping was studied in detail for strongly correlated alloys  $\text{Sm}_{1-x}\text{Eu}_x\text{B}_6$  and  $\text{Yb}_{1-x}\text{Lu}_x\text{B}_{12}$  by photoelectron spectroscopy

<sup>12</sup> Author to whom any correspondence should be addressed.



Content from this work may be used under the terms of the [Creative Commons Attribution 3.0 licence](http://creativecommons.org/licenses/by/3.0/).  
Any further distribution of this work must maintain attribution to the author(s) and the title of the work, journal citation and DOI.

at  $\sim 8000$  eV as well as at 7 and 8.4 eV. It was found that the 4f lattice coherence and intrinsic gap are robust for  $\text{Sm}_{1-x}\text{Eu}_x\text{B}_6$  at least up to the Eu substitution of  $x = 0.15$  while both collapse by Lu substitution already at  $x = 0.125$  for  $\text{Yb}_{1-x}\text{Lu}_x\text{B}_{12}$ . As for the temperature dependence of the spectral shapes near the Fermi level at low temperatures, rather contrasting results were observed between  $\text{YbB}_{12}$  and  $\text{SmB}_6$ . Although the gap shape does not change below 15 K for  $\text{YbB}_{12}$  with the characteristic temperature  $T^*$  of 80 K, the spectral shape of  $\text{SmB}_6$  with a  $T^*$  of 140 K shows that the peak beyond the gap is further increased below 15 K. The temperature dependence of the spectra near the intrinsic gap is clearly different between  $\text{SmB}_6$  and  $\text{YbB}_{12}$ , although both materials have so far been categorized in the same kind of strongly correlated semiconductor. The possibility of the surface contribution is discussed for  $\text{SmB}_6$ .

## Contents

<b>1. Introduction</b>	<b>2</b>
<b>2. Experimental</b>	<b>4</b>
<b>3. Results and discussion</b>	<b>4</b>
<b>4. Conclusions</b>	<b>11</b>
<b>Acknowledgments</b>	<b>11</b>
<b>References</b>	<b>11</b>

## 1. Introduction

Strongly correlated electron systems (SCES) based on rare-earth (RE) elements have attracted wide interest in the last few decades due to their intriguing properties, such as valence-fluctuation (VF), metal–insulator (–semiconductor) transitions and heavy-fermion superconductivity near the quantum critical point. Among them,  $\text{SmB}_6$  [1] and  $\text{YbB}_{12}$  [2, 3] are well known to behave like typical VF semiconductors in a certain low-temperature range. At high temperatures they behave like metals with localized f magnetic moments, whereas a narrow gap opens at the Fermi level ( $E_F$ ) below the characteristic temperature  $T^*$ , which has been reported as  $T^* \sim 140$  K for  $\text{SmB}_6$  [4]<sup>13</sup> and  $T^* \sim 80$  K for  $\text{YbB}_{12}$  [5]. The gaps of single-crystal  $\text{SmB}_6$  and  $\text{YbB}_{12}$  have been discussed from the transport, optical and inelastic neutron scattering (INS) measurements. The so-called hybridization-gap model has been proposed to explain the gap formation. Recently, two types of gaps with different magnitude were reported as the so-called ‘large’ gap ( $\Delta_L \sim 10$ – $20$  meV) and ‘small’ gap ( $\Delta_S \sim 3$ – $7$  meV)<sup>14</sup>, where the latter was thought to take place for the in-gap states formed within the large gap. The in-gap

<sup>13</sup> Except for one ARPES result, most results were obtained on repeatedly scraped or fractured surfaces at  $h\nu = 21.2$  eV.

<sup>14</sup> By optical studies of  $\text{SmB}_6$  [6] combined with other experiments, the ‘large’ gap of  $\Delta_L \sim 19$  meV above 15 K and the ‘small’ gap of  $\Delta_S \sim 3$  meV around 3 K were observed. On the other hand, from the temperature dependence of the electrical resistivity for  $\text{YbB}_{12}$  [5], the magnitudes of the ‘large’ and ‘small’ gaps estimated as twice as large as the activation energy were predicted to be  $\Delta_L \sim 12$  meV for  $15 \text{ K} < T < 40 \text{ K}$  and  $\Delta_S \sim 4$  meV for  $7 \text{ K} < T < 15 \text{ K}$ .

states have been reported in SCES semiconductors (not only  $\text{SmB}_6$  [6]<sup>15</sup> and  $\text{YbB}_{12}$  [7] but also  $\text{Ce}_3\text{Bi}_4\text{Pt}_3$  [8] and  $\text{FeSi}$  [9]). Various theoretical approaches have been proposed to interpret the evolution of the ‘large’ and ‘small’ gaps as well as the VF behavior by means of the Wigner lattice model [10], the exciton–polaron model [11] and the Anderson lattice model at half-filling [12]. Despite numerous experimental and theoretical studies, the origin of the gap states has not been fully clarified yet [13–15].

Photoelectron spectroscopy (PES) is a powerful tool to directly determine the spectral density of states (DOS) as well as quasiparticle band structures. To date, PES studies, using conventional photon energies ( $h\nu \sim 20\text{--}125\text{ eV}$ ), have been performed for  $\text{SmB}_6$  [4] (see footnote 13) and  $\text{YbB}_{12}$  [16, 17]<sup>16</sup>. These conventional PESs have, however, the inherent character of surface sensitivity due to the short inelastic mean-free path (IMFP) of photoelectrons ( $\sim 5\text{ \AA}$ ) [18]. Since the surface of such SCES semiconductors can be metallic [19], more bulk-sensitive PES studies are desired. Recently, hard x-ray PES (HAXPES) has widely been recognized as a highly bulk-sensitive technique because of the long IMFP and applicability to various SCES [20, 21]. The IMFP reaches up to  $\sim 100\text{ \AA}$  at  $h\nu \sim 8\text{ keV}$  [18]. Recently, extremely low-energy ( $h\nu < 10\text{ eV}$ ) PES (ELEPES) with excitations by lasers, synchrotron radiation (SR), or Xe and Kr resonance lines has also become popular as a rather bulk-sensitive ultra-high-resolution technique [22–26]. The IMFP for ELEPES is expected to be comparable with that for HAXPES under certain conditions. Thus, combined HAXPES and ELEPES studies are thought to be extremely useful for revealing intrinsic bulk electronic structures of SCES.

In our HAXPES for the SCES alloys  $\text{Yb}_{1-x}\text{Lu}_x\text{B}_{12}$  [27]<sup>17</sup>, it is concluded that the Yb 4f lattice coherence, being effective for  $x = 0$ , collapses easily by Lu substitution (already at  $x = 0.125$ ). In addition, optical studies have independently shown the gap collapse for  $x = 0.125$  [28]<sup>18</sup>. It is thus deduced that the Yb 4f lattice coherence plays an essential role for the gap formation in pure  $\text{YbB}_{12}$ . In the INS studies [29]<sup>19</sup>, however, it was suggested that the spin gap of  $\sim 10\text{ meV}$  as well as a broad INS peak around  $\sim 38\text{ meV}$  could be driven by the Yb 4f single-site effects because these were robust up to  $x = 0.9$ . A polarized neutron study was later performed on single-crystal  $\text{YbB}_{12}$  between 5 and 125 K [30], where three peaks were observed at  $\sim 14$ ,  $\sim 18$  and  $\sim 40\text{ meV}$  at the L point with the wave number  $\mathbf{q} = (0.5, 0.5, 0.5)$ . The results did not support, however, that the peak at  $\sim 40\text{ meV}$  was due to the single-site effect from its  $\mathbf{q}$  dependence. To fully understand the origin of the gaps in SCES semiconductors, the competition between 4f lattice coherence effects and 4f single-site effects must be carefully studied in various cases. Here, we report on bulk-sensitive HAXPES as well as ELEPES on  $\text{Sm}_{1-x}\text{Eu}_x\text{B}_6$  and  $\text{Yb}_{1-x}\text{Lu}_x\text{B}_{12}$  including their doping and temperature dependence and discuss the changes of their electronic structures.

<sup>15</sup> The gap of  $\sim 3\text{ meV}$  below 15 K was interpreted as being due to an excitation from an additional narrow donor-type band located at  $\sim 3\text{ meV}$  below the bottom of the upper conduction band.

<sup>16</sup> Measurements at  $h\nu = 21.2$  and  $40.8\text{ eV}$  were performed on scraped surfaces of single crystals.

<sup>17</sup> The peak at  $\sim 36\text{ meV}$  in  $\text{YbB}_{12}$  was interpreted as being due to the Kondo resonance peak. However, the temperature dependence of its peak energy is beyond the prediction by the single-impurity Anderson model.

<sup>18</sup> For  $\text{YbB}_{12}$ , the optical conductivity spectrum showed a clear energy gap with an onset at  $\sim 20\text{ meV}$  and a shoulder at  $38\text{ meV}$ . With the increase of  $x$  in  $\text{Yb}_{1-x}\text{Lu}_x\text{B}_{12}$ , the gap is rapidly collapsed leaving a shoulder at  $\sim 40\text{ meV}$ .

<sup>19</sup> Spin gap is defined as the energy threshold below which no magnetic signal can be detected in INS.

## 2. Experimental

Single crystals of  $\text{Sm}_{1-x}\text{Eu}_x\text{B}_6$  (cubic  $\text{CaB}_6$  type:  $x = 0, 0.15$  and  $0.5$ ) [31] and  $\text{Yb}_{1-x}\text{Lu}_x\text{B}_{12}$  (cubic  $\text{UB}_{12}$  type:  $x = 0$  and  $0.125$ ) [5] were grown by Al-flux and floating-zone methods. HAXPES measurements were performed with SR ( $h\nu \sim 8 \text{ keV}$ ) at BL19LXU of SPring-8 [32], using an MBS A1-HE spectrometer. ELEPES measurements were performed with SR ( $h\nu = 7 \text{ eV}$ ) using an MBS A1 spectrometer at BL7U of UVSOR-II [33], as well as with an RF-excited MBS T-1 electron cyclotron resonance lamp (Xe I resonance line:  $h\nu = 8.4 \text{ eV}$ ) and a SCIENTA SES2002 spectrometer at Osaka University [25, 26]. Clean surfaces were obtained by *in situ* fracturing of single crystals in an ultra-high vacuum with a base pressure of  $\sim 5 \times 10^{-8} \text{ Pa}$ . The sample quality of the alloys was checked by the absence of the O 1s signals in HAXPES for all samples. The energy calibration was performed with the Au Fermi edge at each temperature. The total-energy resolution was set to  $120 \text{ meV}$  for  $\text{Sm}_{1-x}\text{Eu}_x\text{B}_6$  and  $65 \text{ meV}$  for  $\text{Yb}_{1-x}\text{Lu}_x\text{B}_{12}$  [27] (see footnote 17) in HAXPES and  $6 \text{ meV}$  for both systems in ELEPES.

## 3. Results and discussion

Figure 1(a) shows the doping dependence of the HAXPES spectra at 20 and 200 K for  $\text{Sm}_{1-x}\text{Eu}_x\text{B}_6$  with  $x = 0, 0.15$  and  $0.5$ . For comparison, the results of  $\text{Yb}_{1-x}\text{Lu}_x\text{B}_{12}$  with  $x = 0$  and  $0.125$  are also reproduced from [27] (see footnote 17) in figure 1(b). At  $h\nu \sim 8 \text{ keV}$  the photoionization cross sections [34] of Sm and Yb 4f states are higher than those of B 2sp and RE 5d states. Therefore, the spectra near  $E_F$  at  $h\nu \sim 8 \text{ keV}$  are dominated by the excitations  $f^6 \rightarrow f^5$  for  $\text{Sm}^{2+}$  ( $4f^6$ ) and  $f^{14} \rightarrow f^{13}$  for  $\text{Yb}^{2+}$  ( $4f^{14}$ ) states<sup>20</sup>. The broad peaks for  $\text{Sm}_{1-x}\text{Eu}_x\text{B}_6$  consist of the Sm  $4f^5$  ( $^6\text{H}_{5/2}$  and  $^6\text{H}_{7/2}$ ) final-state multiplets [35] (vertical line spectra in figure 1(a)), whereas the single peaks for  $\text{Yb}_{1-x}\text{Lu}_x\text{B}_{12}$  are ascribed to the Yb  $4f_{7/2}^{13}$  final state. In figure 1(a), the Sm  $4f^5$  peaks for  $x = 0$  and  $0.15$  in  $\text{Sm}_{1-x}\text{Eu}_x\text{B}_6$  clearly show the energy shift toward  $E_F$  on going from 200 to 20 K in contrast to the negligible shift for  $x = 0.5$ , when the spectra were fitted with Lorentzian (for the slight lifetime broadening) and Gaussian (for the instrumental resolution) broadened functions as shown by the solid lines. The relative intensity and energy for the Sm 4f multiplets were properly taken into account [35].

The estimated Sm 4f peak shift toward  $E_F$  on cooling for  $x = 0$  and  $0.15$  is  $\sim 40 \text{ meV}$ , while that for  $x = 0.5$  is less than  $10 \text{ meV}$  in  $\text{Sm}_{1-x}\text{Eu}_x\text{B}_6$ . On the other hand, the Yb 4f peak shift toward  $E_F$  is  $\sim 20 \text{ meV}$  for  $x = 0$  whereas it is at most  $10 \text{ meV}$  for  $x = 0.125$  in  $\text{Yb}_{1-x}\text{Lu}_x\text{B}_{12}$  (figure 1(b)). As argued previously for  $\text{YbAl}_3$  [36, 37]<sup>21</sup> but not for  $\text{YbInCu}_4$  [38]<sup>22</sup>, peak shifts with temperature of this magnitude are greater than predicted in the single-impurity Anderson model and so are considered to be a 4f lattice coherence effect. The temperature dependence of the 4f peaks observed for  $x = 0$  and  $0.15$  in  $\text{Sm}_{1-x}\text{Eu}_x\text{B}_6$  is qualitatively similar to that for pure  $\text{YbB}_{12}$  and  $\text{YbAl}_3$  in which the Yb 4f lattice coherence is essential for the peak shift.

<sup>20</sup> The  $4f^6$  multiplets from the  $\text{Eu}^{2+}$  ( $4f^7$ ) state for  $\text{Sm}_{1-x}\text{Eu}_x\text{B}_6$  ( $x = 0.15$  and  $0.5$ ) and the  $4f^{13}$  doublets from the  $\text{Lu}^{3+}$  ( $4f^{14}$ ) state for  $\text{Yb}_{1-x}\text{Lu}_x\text{B}_{12}$  ( $x = 0.125$ ) are observed as the localized states in 1–2 and 7–9 eV, and they do not contribute directly to the spectral changes near  $E_F$ .

<sup>21</sup> Negligible thermal shift was observed for the 4f peak ( $4f^{13} J = 7/2$  final state) of  $\text{Yb}_{0.6}\text{Lu}_{0.4}\text{Al}_3$  in contrast to that in  $\text{YbAl}_3$ .

<sup>22</sup> In this case, the 4f peak shift as a smooth function of temperature and the Yb 4f lattice coherence were not discussed because of the bulk valence transition at around 42 K.

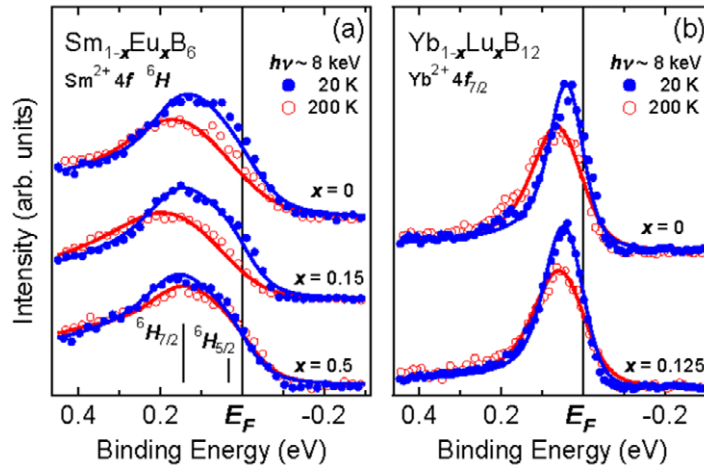


**Figure 1.** HAXPES spectra at 20 and 200 K for (a)  $\text{Sm}_{1-x}\text{Eu}_x\text{B}_6$  in comparison with (b)  $\text{Yb}_{1-x}\text{Lu}_x\text{B}_{12}$  [27] (see footnote 17). The circles and solid lines indicate the experimental data and the fitting results (see text). The spectra are normalized for different  $x$  by the integrated intensity in the binding energy range of  $-0.2 \text{ eV} \leq E_B \leq 0.6 \text{ eV}$  for  $\text{Sm}_{1-x}\text{Eu}_x\text{B}_6$  and  $-0.2 \text{ eV} \leq E_B \leq 0.8 \text{ eV}$  for  $\text{Yb}_{1-x}\text{Lu}_x\text{B}_{12}$  at each temperature.

In this sense, the Sm 4f lattice coherence survives not only for  $x = 0$  but also for  $x = 0.15$  in  $\text{Sm}_{1-x}\text{Eu}_x\text{B}_6$ .

In order to study the relation between the gap formation and the 4f lattice coherence by overcoming the resolution limit of HAXPES, we have performed the ELEPES with much higher energy resolution. The doping- and temperature-dependent ELEPES spectra near  $E_F$  for  $\text{Sm}_{1-x}\text{Eu}_x\text{B}_6$  and  $\text{Yb}_{1-x}\text{Lu}_x\text{B}_{12}$  are presented in figures 2(a) and (b). Here the observed spectra are dominated by the non-RE 4f states, i.e. B 2sp and RE 5d states [34] hybridized with the Sm or Yb 4f states in contrast to the case of HAXPES.

In  $\text{SmB}_6$ , the spectral weight at  $E_F$  decreases clearly and the peak narrows and shifts toward  $E_F$  on decreasing the temperature from 200 to 5 K. The so-called leading edge of the spectra is clearly observed on the occupied state side below  $E_F$ , demonstrating finite gap formation at low temperatures. The spectra show a prominent peak at  $\sim 19 \text{ meV}$  below 15 K. In the surface-sensitive HeI PES spectra on fractured surfaces [4], the background with  $E_B$  above 40 meV is relatively higher than in the present ELEPES spectra and the increase in the peak intensity between 30 and 5.7 K is much smaller than that in ELEPES between 15 and 5 K.

The spectra of  $\text{Sm}_{1-x}\text{Eu}_x\text{B}_6$  with  $x = 0.15$  measured at  $h\nu = 7 \text{ eV}$  show rather similar temperature dependence to that of  $\text{SmB}_6$  except for the peak energy positions while the spectra for  $x = 0.5$  show a typical metallic thermal behavior even at low temperatures without a prominent peak and gap opening. The prominent peak for  $x = 0.15$   $\text{Sm}_{1-x}\text{Eu}_x\text{B}_6$  at low temperatures has also been observed at the same binding energy in several other spectra measured at  $h\nu$  between 7 and 12 eV (not shown here). The bulk origin of this peak is confirmed by the increase of its intensity on decreasing  $h\nu$  as  $12 \rightarrow 9.7 \rightarrow 8.4 \rightarrow 7 \text{ eV}$  in accordance with the increase in the IMFP or bulk sensitivity. The relative increase of this peak intensity compared with the intensity above  $E_B \sim 50 \text{ meV}$  after slight *in situ* surface degradation over 20 h under  $\sim 7 \times 10^{-8} \text{ Pa}$  at  $h\nu = 7$  and 17 eV also supports the bulk origin of this prominent peak. In transport



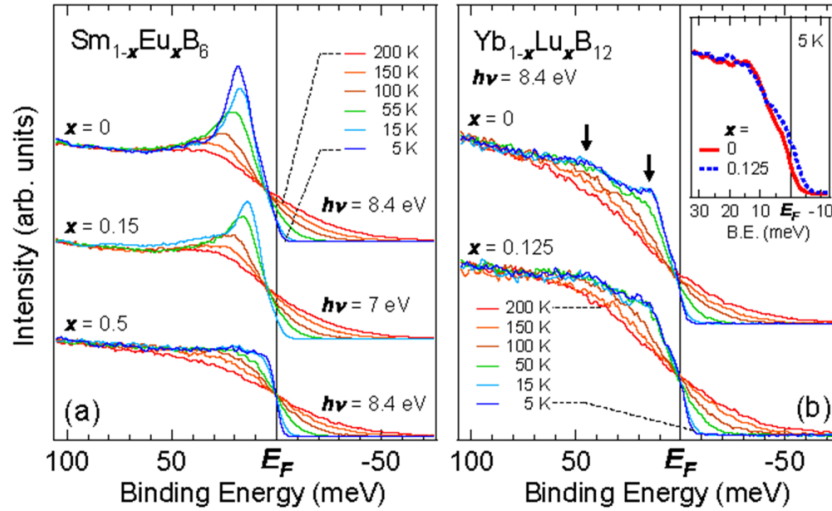


**Figure 2.** Temperature-dependent ELEPES spectra for (a)  $\text{Sm}_{1-x}\text{Eu}_x\text{B}_6$  and (b)  $\text{Yb}_{1-x}\text{Lu}_x\text{B}_{12}$ . The inset of (b) describes the doping dependence of the spectra for  $\text{Yb}_{1-x}\text{Lu}_x\text{B}_{12}$  at 5 K. The intensity of all these spectra is normalized at  $E_B = 100\text{--}120$  meV, where the spectra show no temperature dependence in both systems.

measurements, an exponential increase in the electrical resistivity due to the gap formation on cooling has been observed for  $x \leq 0.2$   $\text{Sm}_{1-x}\text{Eu}_x\text{B}_6$  [39]<sup>23</sup>, consistent with the present ELEPES results.

In the case of  $\text{YbB}_{12}$ , the spectra show a slight but still noticeable decrease of the intensity at  $E_F$  upon cooling, suggesting gap formation (figure 2(b)), where two peaks are observed at 15 and 45 meV at low temperatures (indicated by arrows), being qualitatively similar to the previous work by SR at  $h\nu = 15.8$  eV [40]. For the Lu doping up to  $x = 0.125$ , the two peaks are located at almost the same positions. However, a clear difference between  $x = 0$  and 0.125 is seen at 5 K as shown in the inset of figure 2(b) as the intensity around  $E_F$  is definitely higher for  $x = 0.125$ , suggesting a collapse of the ‘small’ energy gap.

A clear feature to be noted here is a different temperature dependence between  $\text{SmB}_6$  and  $\text{YbB}_{12}$  in the range of 5–15 K, which are far below the characteristic temperature  $T^*$ . Namely, the spectral weight of the narrow peak is further enhanced from 15 to 5 K for  $\text{SmB}_6$  ( $T^* \sim 140$  K) while such a temperature dependence is absent for  $\text{YbB}_{12}$  ( $T^* \sim 80$  K) as more clearly seen later in figures 3(c) and (f). These contrasting results require some new scenario to interpret the results of  $\text{SmB}_6$  since the electronic state of  $\text{YbB}_{12}$  is almost in the ground state at 15 K ( $T^* \sim 80$  K), whereas that of  $\text{SmB}_6$  appears to be not in the ground state even at 15 K ( $T^* \sim 140$  K).  $\text{Sm } 2p_{3/2}$  ( $L_3$ ) edge absorption spectra of  $\text{SmB}_6$  were recently reported [41], where the Sm valence was found to slightly increase toward 3+ below 15 K on decreasing the temperature. Under this condition, the 4f occupation number may decrease and the  $4f^5$  PES final state intensity may also decrease. (As already mentioned, the observed peak in ELEPES is due to the B 2sp and Sm 5d state hybridized with the Sm 4f state. So the peak intensity near the Fermi level does not directly reflect the Sm 4f weight in contrast to HAXPES [42].)

<sup>23</sup> A charge gap is observed up to  $x = 0.4$  in  $\text{Sm}_{1-x}\text{Eu}_x\text{B}_6$ .

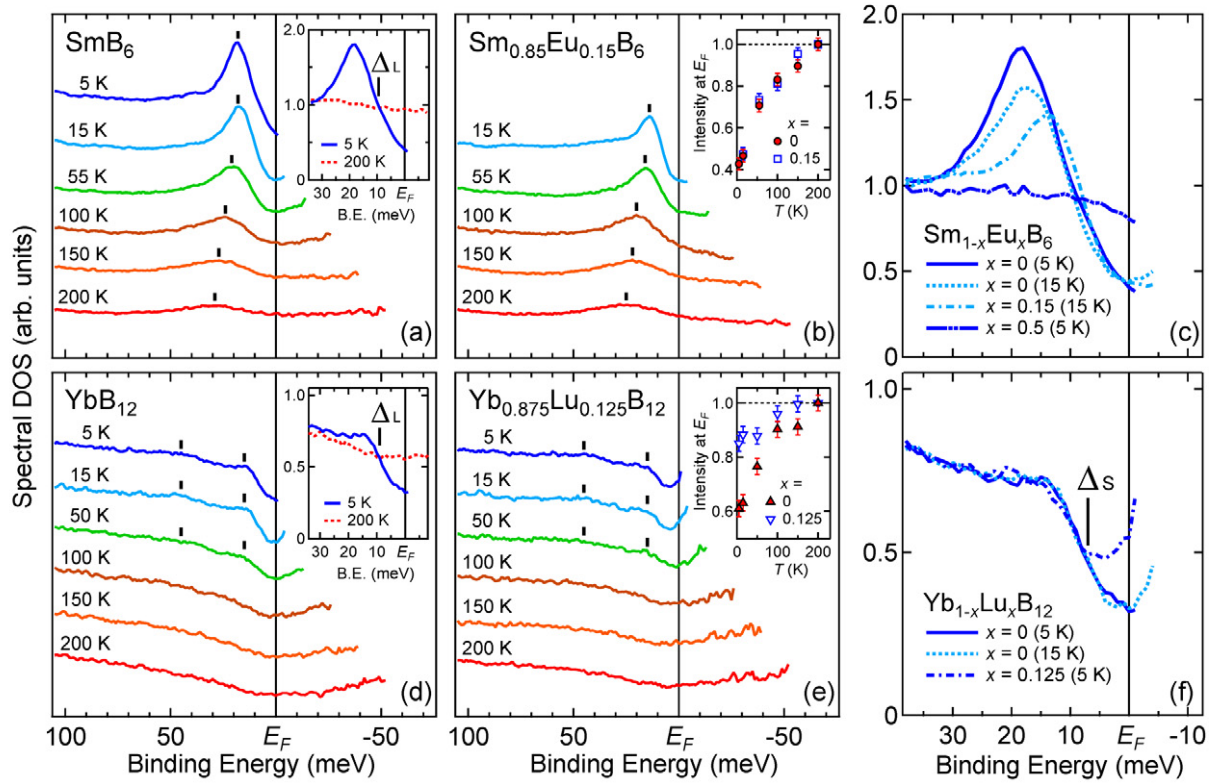


**Figure 3.** Temperature-dependent DOS of  $\text{Sm}_{1-x}\text{Eu}_x\text{B}_6$  for (a)  $x = 0$  at  $h\nu = 8.4\text{ eV}$  and (b)  $x = 0.15$  at  $h\nu = 7\text{ eV}$  and  $\text{Yb}_{1-x}\text{Lu}_x\text{B}_{12}$  for (d)  $x = 0$  and (e)  $x = 0.125$  both at  $h\nu = 8.4\text{ eV}$ . The inset of (a) and (d) shows the comparison of the DOS between 5 and 200 K for  $\text{SmB}_6$  and  $\text{YbB}_{12}$ . The insets of (b) and (e) show the temperature dependence of the spectral intensity at  $E_F$  for  $\text{Sm}_{1-x}\text{Eu}_x\text{B}_6$  and  $\text{Yb}_{1-x}\text{Lu}_x\text{B}_{12}$ , where the value of the intensity at each temperature is normalized by that at 200 K. Some details of the doping dependence of the DOS at low temperatures are shown for (c)  $\text{Sm}_{1-x}\text{Eu}_x\text{B}_6$  and (f)  $\text{Yb}_{1-x}\text{Lu}_x\text{B}_{12}$ .

Although a negative sign of the linear expansion coefficient was reported by thermal expansion measurement [43], its magnitude decreased rapidly below 40 K and became almost negligible below 15 K. Then the presently observed intensity increase of the narrow peak in  $\text{SmB}_6$  around 19 meV between 15 and 5 K cannot be explained. The increase in the intensity of the lowest  $E_B$  peak in ELEPES between 15 and 5 K needs an advanced interpretation beyond these two experimental findings.

For discussions on the doping and temperature dependence of the gap behaviors and peak structures, the DOS information has been obtained by dividing the spectra by the Fermi–Dirac distribution function convoluted with the instrumental resolution. The results are displayed in figure 3, where we show the DOS up to  $3k_B T$  above  $E_F$  keeping high enough statistics. In  $\text{SmB}_6$ , the gap is tentatively estimated to be  $\sim 10\text{ meV}$  from the energy difference between  $E_F$  and the intersection point of the two spectra at 5 and 200 K ( $\Delta_L$  as indicated in the inset of figure 3(a)). This method for evaluating the gap is not considered to be unique, but was taken tentatively because it was a rather straight way to evaluate the rough magnitude of the gap. This energy may correspond to the ‘large’ gap obtained by other experiments (see footnotes 14 and 15) [6, 19].



In the DOS at 5 K we cannot notice any additional structure such as the in-gap state, although the data are of much higher statistics than other results so far reported. The spectral intensity at  $E_F$  is found to be gradually suppressed from around  $T^* \sim 140$  K to lower temperatures for both  $x = 0$  and 0.15 as shown together in the inset of figure 3(b). In the surface-sensitive results [4] (see footnote 13), a similar gap opening was observed below  $\sim 100$  K. The temperature dependence for  $\text{Sm}_{1-x}\text{Eu}_x\text{B}_6$  with  $x = 0.15$  is essentially equivalent to that for  $x = 0$ , whereas the intensity at  $E_F$  stays constant for  $x = 0.5$  (as already shown at the bottom in figure 2(a)).

Therefore, one can safely conclude from figures 3(a) and (b) as well as the inset of figure 3(b) that not only the ‘large’ gap but also the ‘small’ gap do not collapse in  $x = 0.15$   $\text{Sm}_{1-x}\text{Eu}_x\text{B}_6$  even at 100 K. The non-observation of the possible in-gap state at  $\sim 3$  meV below 15 K for  $\text{SmB}_6$  in our ELEPES may be most probably due to the character of its donor-type band excitation [6] (see footnote 15). As shown in figure 3(c), however, the gap (possibly the ‘small’ gap) is collapsed even at 5 K for  $x = 0.5$   $\text{Sm}_{1-x}\text{Eu}_x\text{B}_6$ , consistent with the collapse of the 4f lattice coherence as confirmed by HAXPES shown in figure 1(a). Meanwhile, the peak shifts almost linearly toward  $E_F$  with decreasing temperature for both  $x = 0$  and 0.15 (figures 3(a) and (b)). The observed peak shift and the gap opening behaviors of  $\text{Sm}_{1-x}\text{Eu}_x\text{B}_6$  in the ELEPES can be understood by considering the reduction of the 4f lattice coherence for increased  $x$ .

Meanwhile the DOS of  $\text{Yb}_{1-x}\text{Lu}_x\text{B}_{12}$  for  $x = 0$  and 0.125 is shown in figures 3(d) and (e). For both, the intensity of the broad peaks at  $\sim 15$  and  $\sim 45$  meV reduces with increasing temperature and the peaks are almost smeared out above  $\sim 100$  K. One can see almost no dependences of the peak energies on  $x$  and temperature in ELEPES in contrast to the Kondo resonance peak observed in the bulk-sensitive HAXPES. The crystal electric field splitting in  $\text{YbB}_{12}$  was predicted to be  $\sim 6$  and  $\sim 11$  meV [29] (see footnote 19) and thought not to correspond to the observed structures in the photoelectron spectra. The Kondo peak of  $\text{YbB}_{12}$  was observed at  $\sim 36$  meV in HAXPES at low temperatures below 20 K as shown in figure 1(b). The observed structure in figure 3(d) at  $\sim 45$  meV is not directly representing the Kondo peak with dominant Yb 4f character because of the dramatically decreased relative photoionization cross section of the Yb 4f states at  $h\nu = 8.4$  eV [34]. Although the origins of the observed structures in  $\text{YbB}_{12}$  in photoelectron spectra at  $h\nu$  of 15.8 and 100 eV and INS in the similar energy region were compared and discussed [40, 44], interpretation is still not settled<sup>24</sup>.

The gap of  $\text{YbB}_{12}$  observed in the present ELEPES experiment is tentatively estimated to be  $\sim 10$  meV according to the definition as applied to  $\text{SmB}_6$  (see the inset of figure 3(d)), consistent with the ‘large’ gap reported by the electrical resistivity [5]. As seen in figures 3(d) and 2(b), the intensity at  $E_F$  for  $\text{YbB}_{12}$  decreases upon cooling as indicated by the full (red) triangles in the inset of figure 3(e), where it starts to reduce steeply below 50 K. However, the intensity decrease at  $E_F$  is much less for  $x = 0.125$   $\text{Yb}_{1-x}\text{Lu}_x\text{B}_{12}$  as shown by the empty (blue) triangles in the inset of figure 3(e). The direct comparison of DOS between  $x = 0$  and 0.125 at low temperatures is shown in figure 3(f). It is found that the DOS minimum near  $E_F$  recovers noticeably for  $x = 0.125$  even at 5 K. This energy scale less than  $\sim 7$  meV is comparable with the magnitude of the ‘small’ gap [5]. We conclude that the small gap ( $\Delta_S \leq 7$  meV) collapses even at low temperatures with Lu substitution of  $x = 0.125$ , whereas the large gap ( $\Delta_L \geq 10$  meV) remains still. From the doping dependence of these two gaps for  $\text{Yb}_{1-x}\text{Lu}_x\text{B}_{12}$ , we conclude that

<sup>24</sup> Two peaks were observed at  $\sim 50$  and  $\sim 15$  meV at low temperatures below  $\sim 60$  K at  $h\nu = 15.8$  and 100 eV. The  $\sim 15$  meV peak was interpreted as due to hybridization between the Yb 4f and Yb 5d states in [40]. INS on single-crystal  $\text{YbB}_{12}$  showed spin gap structure with two sharp, dispersive, in-gap excitations at  $\sim 14.5$  and  $\sim 20$  meV. The former peak was ascribed to the short-range correlation near the antiferromagnetic wave vector [44].

the ‘small’ gap collapses when the 4f lattice coherence is broken, while the ‘large’ gap survives in this  $\text{Yb}_{1-x}\text{Lu}_x\text{B}_{12}$  system because it is induced by the 4f single-site effects. The spin gap, robustly detected up to  $x = 0.9$  in the INS for  $\text{Yb}_{1-x}\text{Lu}_x\text{B}_{12}$  [29] (see footnote 19), might have such a character as the presently observed ‘large’ gap.

In the case of  $\text{Sm}_{1-x}\text{Eu}_x\text{B}_6$ , however, not only the ‘large’ gap but also the ‘small’ gap survive up to at least  $x = 0.15$  and up to 50 K, although both gaps are collapsed for  $x = 0.5$  even at 5 K. Although these results are in strong contrast to the collapse of the ‘small’ gap in  $\text{Yb}_{1-x}\text{Lu}_x\text{B}_{12}$  already for  $x = 0.125$  and at 5 K as mentioned above, they are well correlated with the temperature dependence of the 4f HAXPES spectra, which showed the robust 4f lattice coherence as well as the robust intrinsic gap for  $\text{Sm}_{1-x}\text{Eu}_x\text{B}_6$  at least up to  $x = 0.15$  in contrast to the collapse of the 4f lattice coherence for  $\text{Yb}_{1-x}\text{Lu}_x\text{B}_{12}$  already at  $x = 0.125$ . In  $\text{SmB}_6$  Sm atoms and  $\text{B}_6$  clusters have the CsCl structure, whereas in  $\text{YbB}_{12}$  Yb atoms and  $\text{B}_{12}$  clusters have the NaCl structure. Then the lowest Sm and Yb 5d orbitals may have different characters, influencing the hybridization with the 4f states. In addition, the energy positions of the doped Eu and Lu 4f states are different. These effects may influence the  $x$  dependence of the 4f lattice coherence, too.

Within the periodic Anderson model and/or hybridization-gap model [12, 45], the electronic structure of SCES semiconductors is equivalent to that of the usual band insulators at low temperatures due to the renormalization. Therefore, it is expected from these models that the intrinsic gap from the 4f lattice coherence should close at  $E_F$  for SCES semiconductors when the 4f lattice coherence is lost. In addition, these models suggest that the spectral function is independent of temperature in the region well below  $T^*$ . Such features are consistent with the results for  $\text{Yb}_{1-x}\text{Lu}_x\text{B}_{12}$  at  $T \leq 15$  K. However, the latter expectation contradicts the experimental results of  $\text{SmB}_6$  at 15 and 5 K.

Namely, there seems to be another degree of freedom even below 15 K in  $\text{SmB}_6$ . For example, Sm valence increase below 15 K with decreasing temperature was reported by means of really bulk-sensitive and rather impurity-insensitive Sm 2p core absorption [41]. Although the photoemission intensity of the  $4f^4$  final states from the  $\text{Sm}^{3+}$  state could be increased in this case, that of the  $4f^5$  from the  $\text{Sm}^{2+}$  state cannot be increased. Since the peak at  $\sim 19$  meV is to some extent related to the  $\text{Sm } 4f^5(^6\text{H}_{5/2})$  state, the intensity increase of the ELEPES peak near this energy in figure 3(c) below 15 K cannot be explained by this valence change effect. It is natural to think that the change of the electronic structures near 19 meV at low temperature (below 15 K) takes place independently of the change of bulk electronic structures along with or after the intrinsic gap opening with decreasing temperature.

So far high-resolution photoelectron spectroscopy and angle-resolved photoelectron spectroscopy were performed on the single-crystal  $\text{SmB}_6$  surfaces prepared by *in situ* scraping by a diamond file [4, 17] (see footnote 16), fracturing and cleavage [4] or by Ar sputtering followed by annealing [46]. The surface quality of those samples by scraping or sputtering might not be better than the fractured single-crystal surface employed in the present experiment. Although the 4f-dominated  $^6\text{H}_{5/2}$  peak was clearly observed at  $\sim 18$  meV at  $h\nu = 40.8$  eV due to the increased photoionization cross section, the peaks near 15–18 meV with less Sm 4f contribution at  $h\nu = 21.2$  eV [17] (see footnote 16) and 10.6 eV [46] were much weaker than the present results on a fractured surface at  $h\nu = 8.4$  eV, revealing the higher sample surface quality of the present ELEPES than those surfaces. Although the results at  $h\nu = 21.2$  eV on a fractured surface [4] (see footnote 13) provide apparently similar spectral shapes as the present ELEPES, still the temperature dependence is different and the relative height of the lowest  $E_B$

peak is lower than the present ELEPES. The higher surface sensitivity at  $h\nu = 21.2$  eV than at  $h\nu = 8.4$  eV may be a reason why the relative bulk contribution to this peak is weaker at  $h\nu = 21.2$  eV.

As already discussed, the in-gap state at 3–5 meV below the conduction band minimum [47] may not be observable by photoelectron spectroscopy. Another rather commonly observed gap from optical measurements as well as conductivity measurements with a full gap magnitude of  $19 \pm 2$  meV [6] (see footnotes 14 and 15) between 70 and 15 K may be observable around 10 meV in bulk-sensitive photoelectron spectra. But this energy position will rather depend upon the location of the Fermi level in the real system.

In the case of the present ELEPES of SmB<sub>6</sub>, the opening of the bulk ‘large’ gap below 100 K is clear (inset of figure 3(b)). The explanation of the peak intensity increase in SmB<sub>6</sub> from 15 to 5 K is difficult as long as we consider only the valence increase of bulk electronic states [41]. Here one may think of a possible contribution of the surface. The ELEPES, which was often claimed and confirmed to be bulk sensitive, is, however, now known to show noticeable surface sensitivity depending upon the individual materials and experimental conditions, including the binding energies of the probed electronic states [26, 48].

Recently, a theoretical prediction that some of the Kondo insulators (semiconductors) can have a metallic surface and can be classified into a three-dimensional topological insulator has been attracting wide attention [49, 50]. Among them, SmB<sub>6</sub> was proposed to be a promising candidate for a strong topological insulator [51], where metallic surface states were claimed to correspond to the so far not fully explained in-gap states. If such a metallic state induced by the momentum-dependent hybridization between the crystal field split Sm 4f state and conduction electron states takes place on the surface due to the strong spin–orbit coupling on f sites, the surface electronic structures may still have freedom at low temperatures even below 15 K [50]. The increase of the peak intensity at  $\sim 19$  meV below 15 K may somehow be related to this surface state as also discussed in [46]. According to the band calculation in [51], metallic surface states with a Dirac cone are predicted near the surface  $\Gamma$  point and surface X points which are characteristic for the topological insulator. Then spin polarization may be observed for such states. In addition, surface bands with the bottom at the surface X point are predicted [51] extending upward and crossing the Fermi level in the middle region between the surface  $\Gamma$  and X points. The latter bands have a bottom at  $\sim 14$  meV, where the DOS may have a maximum. If the gap opens in the bulk electronic states, the relative spectral weight of the surface electronic states against the bulk electronic states may increase. For example, the surface state was very clearly observed on the Cu(111) surface by angle-resolved ELEPES at  $h\nu \sim 8.4, 10.0$  and  $11.6$  eV [26]. The angle-resolved ELEPES could also resolve the Dirac cone of the surface metallic state of a topological insulator Bi<sub>2</sub>Te<sub>3</sub> [48]. Thus, the ELEPES on SmB<sub>6</sub> might have enabled us to partially probe the DOS of surface states also under the present ELEPES condition. If metallic states are present on the topological insulator surface after the intrinsic gap opening, the surface state may become sensitively observable in the gap energy region below  $E_F$ . So one of the plausible interpretations of the present ELEPES results of SmB<sub>6</sub> at low temperature (15–5 K) is to consider the contribution of this surface state DOS overlapping with the prominent bulk peak in the region of  $\sim 19$  meV. In this scenario, the sharp bulk peak at  $\sim 19$  meV associated with the ‘large’ gap opening will show an intensity increase between 15 and 5 K due to the increase of the background overlapping in this energy region resulting from the surface bands, which become observable with slightly higher intensity by the opening of the gap. For further discussions, spin- and angle-resolved photoelectron spectroscopy with different bulk or surface sensitivity is

necessary. Point-contact spectroscopy [52] as well as scanning tunneling spectroscopy may also be useful for the study of these electronic structures.

#### 4. Conclusions

In conclusion, a combination of ELEPES and bulk-sensitive HAXPES is found to be a very powerful method for studying electronic structures of SCES semiconductors. It is found that the 4f lattice periodicity is essential for the gap formation and collapse in  $\text{Yb}_{1-x}\text{Lu}_x\text{B}_{12}$  in a certain  $x$  range below  $x = 0.125$  and in  $\text{Sm}_{1-x}\text{Eu}_x\text{B}_6$  in a certain  $x$  range below  $x = 0.5$  at low temperatures. Although the electronic ground state is achieved at 15 K in  $\text{YbB}_{12}$  with  $T^* \sim 80$  K, the electronic states are still not in the ground state at 15 K in  $\text{SmB}_6$  with  $T^* \sim 140$  K. Even the bulk valence change below 15 K cannot explain the increase of the intensity of the peak at  $\sim 19$  meV in  $\text{SmB}_6$  below 15 K. The observed unusual behavior of ELEPES spectral shapes in  $\text{SmB}_6$  is thought to be possibly due to the overlap of some surface contribution. Further spin- and angle-resolved high-resolution photoelectron spectroscopy will ascertain the validity of this possible scenario in the near future.

#### Acknowledgments

This work was supported by the Grant-in-Aid for Science Research (18104007, 18684015, 21340101, and Innovative Areas ‘Heavy Electrons’ 20102003) of MEXT, Japan, the Global COE program (G10) of JSPS, Japan, and the KHYS, KIT, Germany. The work at Sogang University was supported by MIST/KRF (2009-0051705) of Korea. A part of the ELEPES study was performed as a Joint Studies Program of the Institute for Molecular Science (2008).

#### References

- [1] Menth A *et al* 1969 *Phys. Rev. Lett.* **22** 295
- [2] Kasaya M *et al* 1983 *J. Magn. Magn. Mater.* **31–34** 437
- [3] Kasaya M *et al* 1985 *J. Magn. Magn. Mater.* **47–48** 429
- [4] Nozawa S *et al* 2002 *J. Phys. Chem. Solids* **63** 1223
- [5] Iga F *et al* 1998 *J. Magn. Magn. Mater.* **177–181** 337
- [6] Gorshunov B *et al* 1999 *Phys. Rev. B* **59** 1808
- [7] Gorshunov B *et al* 2006 *Phys. Rev. B* **73** 045207
- [8] Pietrus T *et al* 2008 *Phys. Rev. B* **77** 115134
- [9] Schlesinger Z *et al* 1993 *Phys. Rev. Lett.* **71** 1748
- [10] Kasuya T 1976 *J. Physique Coll.* **37** C4-261
- [11] Kikoin K A and Mishchenko A S 1995 *J. Phys.: Condens. Matter* **7** 307
- [12] Riseborough P S 2003 *Phys. Rev. B* **68** 235213
- [13] Cooley J C *et al* 1995 *Phys. Rev. Lett.* **74** 1629
- [14] Antonov V N *et al* 2002 *Phys. Rev. B* **66** 165209
- [15] Thunström P *et al* 2009 *Phys. Rev. B* **79** 165104
- [16] Susaki T *et al* 1999 *Phys. Rev. Lett.* **82** 992
- [17] Souma S *et al* 2002 *Physica B* **312–313** 329
- [18] Tanuma S *et al* 2003 *Surf. Interface. Anal.* **35** 268
- [19] Flachbart K *et al* 2001 *Physica B* **293** 417 and references cited therein
- [20] Yamasaki A *et al* 2007 *Phys. Rev. Lett.* **98** 156402

- [21] Suga S *et al* 2009 *New J. Phys.* **11** 103015
- [22] Kiss T *et al* 2005 *Phys. Rev. Lett.* **94** 057001
- [23] Arita M *et al* 2002 *Surf. Rev. Lett.* **9** 535
- [24] Souma S *et al* 2007 *Rev. Sci. Instrum.* **78** 123104
- [25] Funabashi G *et al* 2008 *Japan. J. Appl. Phys.* **47** 2265
- [26] Suga S *et al* 2010 *Rev. Sci. Instrum.* **81** 105111
- [27] Yamaguchi J *et al* 2009 *Phys. Rev. B* **79** 125121
- [28] Okamura H *et al* 2000 *Phys. Rev. B* **62** R13265
- [29] Alekseev P A *et al* 2004 *J. Phys.: Condens. Matter* **16** 2631
- [30] Nemkovski K S *et al* 2007 *Phys. Rev. Lett.* **99** 137204
- [31] Yeo S *et al* 2009 *Appl. Phys. Lett.* **94** 042509
- [32] Yabashi M *et al* 2001 *Phys. Rev. Lett.* **87** 140801
- [33] Kimura S *et al* 2007 *AIP Conf. Proc.* **879** 527
- [34] Yeh J J and Lindau I 1985 *At. Data Nucl. Data Tables* **32** 1
- [35] Cox P A 1975 *Struct. Bond.* **24** 59
- [36] Suga S *et al* 2005 *J. Phys. Soc. Japan* **74** 2880
- [37] Yamaguchi J *et al* 2007 *New J. Phys.* **9** 317
- [38] Suga S *et al* 2009 *J. Phys. Soc. Japan* **78** 074704
- [39] Yeo S *et al* 2012 *Phys. Rev. B* **85** 115125
- [40] Takeda Y *et al* 2006 *Phys. Rev. B* **73** 033202
- [41] Mizumaki M, Tsutsui S and Iga F 2009 *J. Phys. Conf. Ser.* **176** 012034
- [42] Yamaguchi J *et al* 2010 *J. Phys.: Conf. Ser.* **200** 012230
- [43] Mandrus D *et al* 1994 *Phys. Rev. B* **49** 16809
- [44] Mignot J–M *et al* 2005 *Phys. Rev. Lett.* **94** 247204
- [45] Hanzawa K 1998 *J. Phys. Soc. Japan* **67** 3151
- [46] Miyazaki H *et al* 2012 *Phys. Rev. B* **86** 075105
- [47] Gabani S *et al* 2001 *Solid State Commun.* **117** 641
- [48] Plucinski L *et al* 2011 *Appl. Phys. Lett.* **98** 222503
- [49] Dzero M, Sun K, Galitski V and Coleman P 2010 *Phys. Rev. Lett.* **104** 106408
- [50] Dzero M, Sun K, Coleman P and Galitski V 2012 *Phys. Rev. B* **85** 045130
- [51] Takimoto T 2011 *J. Phys. Soc. Japan* **80** 123710
- [52] Flachbart K *et al* 2001 *Phys. Rev. B* **64** 085104